Synthetic Metals 162 (2012) 862–867

Contents lists available at SciVerse ScienceDirect

Synthetic Metals

journal homepage: www.elsevier.com/locate/synmet

Theoretical study on polyaniline gas sensors: Examinations of response mechanism for alcohol

Sha-Sha Liu [a], Li-Jun Bian [a], Feng Luan [a], Meng-Tao Sun [b], Xiao-Xia Liu [a,*]

[a] Department of Chemistry, Northeastern University, Shenyang 110819, China
[b] Beijing National Laboratory for Condensed Matter Physics, Institute of Physics, Chinese Academy of Sciences, Beijing 100190, China

ARTICLE INFO

Article history:
Received 22 September 2011
Received in revised form 18 March 2012
Accepted 23 March 2012

Keywords:
Polyaniline
Gas response
Alcohols
Density functional theory

ABSTRACT

Geometry optimization was conducted on a series of emeraldine salt (ES) oligoanilines $(2x+2)$-ES^+ ($x=0$, 1, 2, 3), alcohols and complexes composed of oligoanilines and alcohols by density functional theory (DFT) method at UB3LYP/6-31g (d) level. Electronic properties of complexes composed by $(2x+2)$-ES^+ oligoanilines with methanol, ethanol, propanol and isopropanol were investigated at higher level UB3LYP/6-311++g (d, p) to model the response of polyaniline (PANI) to alcohols. Influences of oligoaniline chain length and alcohols on the binding properties of the complexes were discussed based on the calculated results.

1. Introduction

Conducting polymers (CPs) including polyacetylene [1], polypyrrole [2], polythiophene [3] and polyaniline [4,5] (PANI) have been widely studied in the fields of organic batteries, optical displays, microelectronics and sensors because of their excellent electrical conductivity, electrochemical activity, environmental stability and etc. [6–9]. Among them, PANI is fascinating because it can be easily synthesized and can favorably respond to guest molecule at room temperature [10–12]. In addition, PANI can be shaped into various nanostructures and so possesses of high surface area to get good contact with guest molecules. Consequently, PANI has been investigated for nanofiber gas sensors in recent years. The gas response mechanisms of PANI have been studied as well [10,13–16]. In 2004, Kaner and Weiller adopted interfacial polymerization method for the synthesis of polyaniline nanofibers and then developed nanofiber sensors [10]. Five response mechanisms corresponding to five kinds of guest gas molecules were proposed by the authors, such as acid doping mechanism for HCl, base dedoping mechanism for NH_3, reduction mechanism for N_2H_4, swelling mechanism for $CHCl_3$, and polymer chain conformation change mechanism for CH_3OH [10]. However, there has been no theoretical study of response mechanisms of PANI to gas molecules although some groups tried to give some explanations from experimental point of view [10,14–16]. Recently, Pinto et al. fabricated a single nanofiber sensor from an electrospun PANI nanofiber doped by camphor sulfonic acid and then tested its electric response to various alcohol vapors, providing a good chance for theoretical study of gas sensing mechanism [16].

In recent years, quantum chemistry methods have made great progresses in studies of electronic and structural properties of CPs [17–26]. In the beginning, semi-empirical methods were the dominant theoretical tool to study PANI polymer [17,18,27]. The modified neglect of differential overlap (MNDO) technique and the Austin model 1 (AM1) method were used to simulate geometries, electronic and optical properties of three base forms of PANI, i.e., leucoemeraldine base (LEB), pernigraniline base (PB) and emeraldine base (EB). Geometries of EB chains were described as an alternated "copolymer" of LEB and PB, in which the LEB units were interconnected by quinoid moieties [27]. It was predicted through geometrical optimizations, energies and proton affinity calculations that the *p*-aminodiphenylamine was preferably protonated on the amine nitrogen between the phenyl rings. Brédas and coworkers elucidated that the optical transitions of three neutral aniline oligomers involving LEB, PB and EB were not significantly modified by the increases of chain length, due to the decrease of π delocalization of the molecular orbitals induced by steric effects and by the incorporation of nitrogen atoms interconnecting the adjacent phenylene rings [27].

Recently, more and more theoretical papers have been published concerning oligonanilines and/or PANI by means of ab initio or density functional theory (DFT) methods [24,28–33]. Geometric and electronic structures of various neutral aniline oligomers were studied by Lim et al. by Restricted Hartree–Fock (RHF) and DFT

* Corresponding author.
E-mail address: xxliu@mail.neu.edu.cn (X.-X. Liu).

0379-6779/$ – see front matter © 2012 Elsevier B.V. All rights reserved.
http://dx.doi.org/10.1016/j.synthmet.2012.03.015

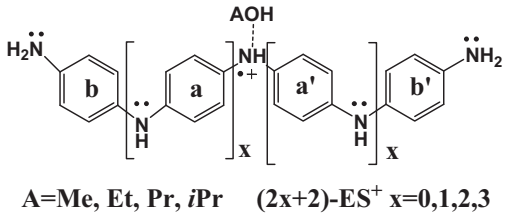

Scheme 1. The interaction between $(2x+2)$-ES$^+$ ($x=0, 1, 2, 3$) and AOH (A = methanol (Me), ethanol (Et), propanol (Pr) and isopropanol (*i*Pr)).

calculations [32]. The energies of DFT-optimized structures are all lower than those of RHF-optimized ones, while the DFT calculated results are in good agreement with experimental observations. A comprehensive theoretical study by Alemán and Casanovas et al. provided an insight into different forms of oligonanilines and found that the EB form was built by repeating units containing amine and imine nitrogen [26]. In addition, the molecular structures and band gaps of LEB, PB and EB forms of PANI were simulated based on their differences in the conjugation of the C_6H_4 rings.

More recently, theoretical chemists were interested in the structure and electronic properties of PANI doped by guest molecules or substituents on backbone of polymer [34–39]. Sein made great efforts to explain effects of substituents in aniline oligomers. They studied the effects of replacing terminal amino groups by hydroxyl groups and found that the hydroxyl terminated aniline trimer had a larger calculated electron affinity than the corresponding amino terminated aniline trimer [39]. Because a larger electron affinity in the salt form of PANI is in favor of good corrosion inhibition, these calculations suggested a new and superior material for anticorrosion. A fascinating work concerning DFT-based electronic structure calculations on a series of PANI complexes to model the hydrogen bonding present in sulfonic acid-doped PANI were performed by Casanovas et al. [40]. Both the geometry and electronic configuration were rearranged, which indicated that a hydrogen bond was constructed between the N—H group in the PANI and the O—S group in the sulfonic acid.

Despite profound theoretical work and publications of excellent papers concerning structural and electronic properties of PANI and/or doped PANI, the exact nature of PANI response mechanism for alcohol molecules is still not completely understood. Therefore, it is necessary to elucidate the PANI response mechanism for alcohol molecules from theoretical point of view. Herein, we preformed a DFT study on a series of complexes designed to model the interaction between individual oligoanilines and different alcohol molecules. Based on calculations we attempted to explain the PANI response mechanism for alcohols.

2. Methods

2.1. Molecular description

According to oxidation states, PANI exists in three forms: LEB denotes fully reduced form, PB represents fully oxidized form and EB is half oxidized form [8]. When doped with acids, nitrogen in PANI-EB chain can be protonated to afford conducting emeraldine salt (ES) form which shows high conductivity because of extensive π conjugation in the polymer chain. In this work, we mainly investigated electronic and structural properties of ES, and effect of interacted alcohol molecules. Radical cation ES oligoanilines with two, four, six and eight benzene rings ended by nitrogen atoms are represent by $(2x+2)$-ES$^+$ ($x=0, 1, 2, 3$) (in Scheme 1). Alcohol molecules used in this work were methanol (Me), ethanol (Et), propanol (Pr) and isopropanol (*i*Pr), which correspond to A = Me, Et, Pr, *i*Pr in Scheme 1, respectively. The response mechanism of

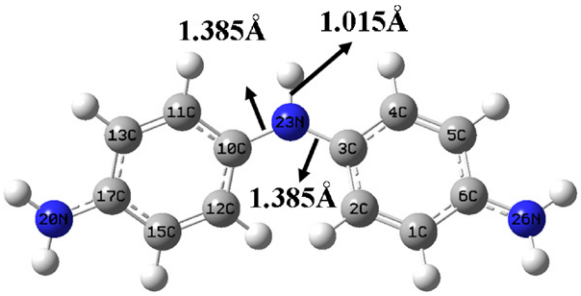

Fig. 1. Optimized geometry of 2-ES$^+$ oligoaniline calculated at UB3LYP/6-31G (d) (bond lengths in Å). C and N atoms are labeled in the molecule.

alcohols to PANI was considered by approaching alcohols to the center of radical cation ES oligoanilines and then full geometry optimizations were carried out. Herein, ES oligoanilines with one reactive center were adopted to simplify the calculated model.

2.2. Computational methods

All geometries were optimized with DFT, Becke's three-parameter exchange functional with the correlation functional of Lee-Yang-Parr (UB3LYP) along with standard 6-31g (d) basis set [41,42]. No imaginary frequencies were found for all optimized structures, which indicated that the calculated structures for $(2x+2)$-ES$^+$ oligoanilines and alcohol-$(2x+2)$-ES$^+$ ($x=0, 1, 2, 3$) complexes are stable. To further investigate molecular properties, we preformed interaction energies and atomic charges calculations at higher level UB3LYP/6-311++g (d, p) on the basis of optimized geometries mentioned above. In quantum chemistry, calculations of molecular properties are susceptible to basis set superposition error (BSSE) if finite basis sets are used. As atoms of interacting molecules approach one another, their basis functions overlap. In the counterpoise method [43] (CP), the BSSE is calculated by re-performing all the calculations using the mixed basis sets, and the error is then subtracted a posteriori from the uncorrected energy. Based on optimized structures, natural bond order (NBO) [44–46] analysis was carried out to investigate charge distribution between ES oligoanilines chain and alcohol molecules. In NBO analysis, the input atomic orbital basis set is transformed via natural atomic orbitals (NAOs) and natural hybrid orbitals (NHOs) into natural bond orbitals (NBOs). All the quantum chemical calculations were performed with Gaussian 09 suite [47].

3. Results and discussion

3.1. Geometric properties of emeraldine salt

Geometry optimizations of oligoanilines $(2x+2)$-ES$^+$ ($x=0, 1, 2, 3$) were carried out at the UB3LYP/6-31g (d) level. Typical optimized structure (2-ES$^+$) is shown in Fig. 1. Optimized geometric parameters (bond lengths in Å and bond angles in deg) are summarized in Table 1.

Table 1
Geometric parameters of $(2x+2)$-ES$^+$ ($x=0, 1, 2, 3$) including $d_{N_{23}\cdots H}$ in Å, the angle $\angle C_{10}N_{23}C_3$, the dihedral angle $\angle C_2C_3N_{23}C_{10}$ and the torsion angle of two adjacent phenyl rings *T* in deg, respectively. Refer to Fig. 1 for atomic labels.

x	$d_{N_{23}\cdots H}$	$\angle C_{10}N_{23}C_3$	$\angle C_2C_3N_{23}C_{10}$	T
0	1.015	130.9	−22.47	37.83
1	1.013	130.7	−22.57	38.03
2	1.012	130.3	−23.19	39.02
3	1.011	129.9	−24.17	40.68

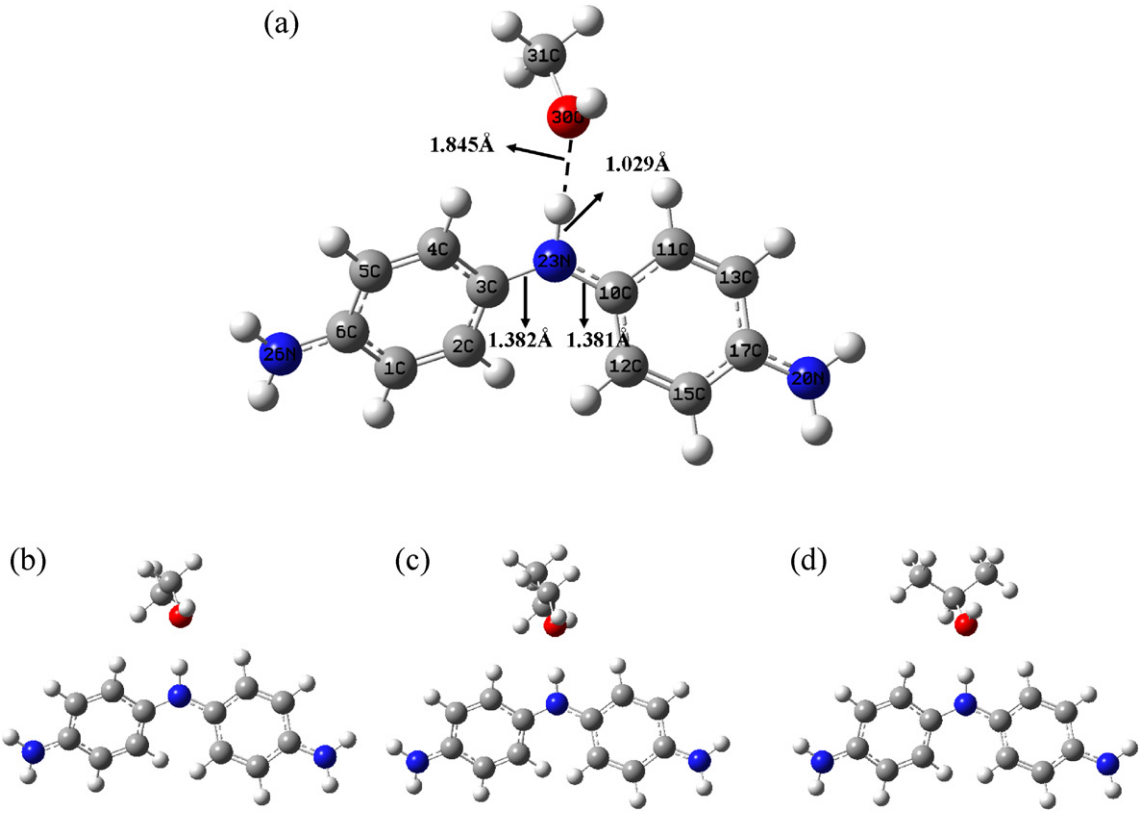

Fig. 2. Optimized molecule geometries of (a) methanol-2-ES$^+$, (b) ethanol-2-ES$^+$, (c) propanol-2-ES$^+$ and (d) isopropanol-2-ES$^+$ complexes calculated at UB3LYP/6-31G (d) level. C, N and O atoms are labeled in (a).

As can be seen in Table 1, geometric parameters vary with the increase of phenyl ring in (2x + 2)-ES$^+$ (x = 0, 1, 2, 3). The bond length $d_{N_{23}\cdots H}$ and the angle $\angle C_{10}N_{23}C_3$ gradually decrease along with the increase of phenyl ring number. The bond length $d_{N_{23}\cdots H}$ decreases 0.004 Å when the phenyl ring number increases from 2 in 2-ES$^+$ to 8 in 8-ES$^+$. The angle $\angle C_{10}N_{23}C_3$ decreases 1° from 2-ES$^+$ to 8-ES$^+$. However, the dihedral angle $\angle C_2C_3N_{23}C_{10}$ gradually increases from −22.47° to −24.17° as phenyl ring number in oligoaniline increases from 2 to 8. The torsion angle T, which is described the torsion degree of two adjacent phenyl rings in center of (2x + 2)-ES$^+$ (x = 0, 1, 2, 3) chain, greatly increases as oligoaniline chain increases. The torsion angle T increases 2.85° from 2-ES$^+$ to 8-ES$^+$, which result in hindrance for electron transfer along the oligoanilines. The conjugation is weakened along with the increase of oligoaniline chain due to the increase in torsion angle T and dihedral angle $\angle C_2C_3N_{23}C_{10}$, and so results in the decrease in N_{23}—H bond length.

3.2. Structural and electronic properties of alcohol-2-ES$^+$ complexes

To investigate the response of 2-ES$^+$ to alcohols, we studied the structural and electronic properties of complexes built by 2-ES$^+$ and methanol, ethanol, 1-propanol, and isopropanol, respectively. All geometries of alcohol-2-ES$^+$ complexes were optimized at UB3LYP/6-31g (d) level and shown in Fig. 2. The intramolecular and intermolecular geometric parameters $d_{O\cdots H}$, ∠NH…O and $\angle C_2C_3N_{23}C_{10}$, and data of the interaction energies, ΔE_{int} and $\Delta E_{int,cp}$ are listed in Table 2. Herein, interaction energies and atomic charges were calculated at UB3LYP/6-311++g (d, p) level.

An ion–dipole force is an attractive force that results from the electrostatic attraction between an ion and a neutral molecule that has a dipole [48–50]. In Me-2-ES$^+$ complex, a cation oligoaniline 2-ES$^+$ attracts the partially negative end of a neutral polar methanol. The binding energy is −29.7 kcal/mol for Me-2-ES$^+$ complex, indicating the ion–dipole interaction is formed between oligoaniline and methanol. This is further supported by the values of $d_{O\cdots H}$ (1.845 Å) and ∠NH…O (180°) in the complex. As a result of ion–dipole interaction, the bond lengths of N—H in 2-ES$^+$ and O—C in methanol increase 0.014 Å and 0.006 Å, respectively. Due to the ion–dipole interaction, the dihedral angle between two phenyl rings decreases about 0.9°, which will influence the electronic property of the oligoaniline. Charge transfer between methanol and 2-ES$^+$ was investigated by Mulliken charges distribution ($Q_{MULLIKEN}$) and NBO atomic charges (Q_{NBO}) in Me-2-ES$^+$ complex (see Table 2). It can be seen from Table 2 that the ion–dipole interaction involves a net charge transfer from methanol to 2-ES$^+$ of 0.034 e$^-$ based on Q_{NBO} and 0.020 e$^-$ based on $Q_{MULLIKEN}$.

The size effect of alcohols on their complexes with 2-ES$^+$ were considered involving methanol, ethanol and 1-propanol (n = 0, 1, 2 in Scheme 1) and the results are summarized in Table 2. From Table 2, ∠NH…O decreases from 180° as hydrocarbon H in methanol is replaced by alkyl. Although the bond length $d_{O\cdots H}$ is not obviously influenced by the increase of chain length in alcohol, the Mulliken charges distribution ($Q_{MULLIKEN}$) and NBO atomic charges (Q_{NBO}) increase from Me-2ES$^+$ to Et-2ES$^+$ and Pr-2ES$^+$ due to the electron donating of alkyl group.

The structural and binding properties of iPr-2-ES$^+$ complex are obviously different from those linear chain alcohol counterpart Pr-2-ES$^+$ complex (see Table 2). The iPr-2-ES$^+$ complex has a shorter bond $d_{O\cdots H}$ and is more stable ($d_{O\cdots H}$ = 1.837 Å, ΔE_{int} = −12.2 kcal/mol and $\Delta E_{int,cp}$ = −11.5 kcal/mol) than Pr-2-ES$^+$ complex due to the appearance of two methyl groups in isopropanol molecule. As known, the net electrostatics effect of alkyl is controlled by the competition of hyperconjugation and inductive

Table 2
Optimized geometric parameters between alcohol and 2-ES$^+$ ($d_{O\cdots H}$ in Å, ∠N—H…O, the dihedral angle $\angle C_2C_3N_{23}C_{10}$ and the torsion angle T in deg, respectively) obtained at UB3LYP/6-31g (d) level, noncorrected and couterpoise corrected interaction energies (ΔE_{int} and $\Delta E_{int,cp}$ in kcal/mol), NBO and ESP charges of compounds obtained at UB3LYP/6-311++g (d, p) level. Refer to Fig. 2(a) for atomic labels.

	$d_{O\cdots H}$	∠NH…O	ΔE_{int}	$\Delta E_{int,cp}$	Q_{NBO}	$Q_{MILLKEN}$	$\angle C_2C_3N_{23}C_{10}$	T
Methanol	1.845	180.0	−30.6	−29.7	0.034	0.020	−21.58	35.24
Ethanol	1.847	178.5	−11.6	−10.8	0.036	0.022	−22.32	35.30
1-Propanol	1.845	177.7	−11.8	−11.0	0.039	0.023	−21.74	34.83
2-Propanol	1.837	178.8	−12.2	−11.5	0.036	0.011	−22.34	35.45

effects. When there is an increase of one methyl group in the alkyl chain, the electron cloud is delocalized by forming σ–π or σ–p hyperconjugation. Therefore, two methyl groups in isopropanol act as electron donor. On the other hand, methyl group should be electron acceptor in isopropanol from the inductive effect perspective. However, the hyperconjugation effect should be dominant when one more methyl group is substituted for hydrogen atom in ethanol to produce isopropanol. Shorter bond $d_{O\cdots H}$ establishes between 2-ES$^+$ and the isopropanol and more stable complex forms. This is also supported by both of Mulliken and NBO charge analyses. The charge transference from isopropanol to 2-ES$^+$ oligoanilines increases along with one more methyl group added into ethanol molecule. Therefore, the hyperconjugation effect of two methyl side chains is prior to one alkyl chain from electron donor view.

The dihedral angel $\angle C_2C_3N_{23}C_{10}$ and the torsion angle T in 2-ES$^+$ change slightly upon forming complexes with alcohols. The values of dihedral angle $\angle C_2C_3N_{23}C_{10}$ decrease 0.13 to 0.89° while those of the torsion angle T decrease 2.38 to 3.00° when 2-ES$^+$ oligoanilines form complexes with the alcohols, indicating that the adjacent phenyl rings in 2-ES$^+$ are more coplanar. So the electron transport is easier along the 2-ES$^+$ chain. This is consistent with the experimental results obtained by Pinto et al. that the resistance of a single nanofiber of PANI oligoanilines decreases upon exposure to alcohol molecules [16].

3.3. *Influence of oligoanilines chain length on alcohol-(2x + 2)-ES$^+$ complexes*

In order to investigate the influence of oligoanilines chain length on interactions of methanol, ethanol, propanol and isopropanol with (2x + 2)-ES$^+$, a series of Me-(2x + 2)-ES$^+$, Et-(2x + 2)-ES$^+$, Pr-(2x + 2)-ES$^+$ and *i*Pr-(2x + 2)-ES$^+$, complexes are calculated at UB3LYP/6-31g (d) level. Molecular properties, such as interaction energies or atomic charges are calculated at UB3LYP/6-311++g (d, p) level.

Binding properties of Me-2-ES$^+$, Me-4-ES$^+$, Me-6-ES$^+$ and Me-8-ES$^+$ are summarized in Table 3 and the optimized structure of Me-8-ES$^+$ is shown in Fig. 3. Based on the calculated results (Table 3), the bond length $d_{O\cdots H}$ is the parameter which is significantly influenced by the chain length. The bond length $d_{O\cdots H}$ increase 0.034, 0.057 and 0.075 Å for Me-4-ES$^+$, Me-6-ES$^+$ and Me-8-ES$^+$, respectively, compared to that of Me-2-ES$^+$. Due to increase in bond length $d_{O\cdots H}$, the charge transfer between the methanol and oligoanilines reduce 0.004, 0.008 and 0.009 units of electron for Me-4-ES$^+$, Me-6-ES$^+$ and Me-8-ES$^+$, respectively, based on Q_{NBO} (Table 3). Note that, Mulliken charge distribution is following the same trends with NBO distribution and the concordance between $Q_{MULLIKEN}$ and Q_{NBO} is very remarkable. The energetic stability of complexes obviously decreases due to the enlargement of $d_{O\cdots H}$. The values of ΔE_{int} ($\Delta E_{int,cp}$) are 2 kcal/mol (2 kcal/mol), 3.3 kcal/mol (3.3 kcal/mol) and 4.2 kcal/mol (4.2 kcal/mol) larger than that of Me-2-ES$^+$ complex for Me-4-ES$^+$, Me -6-ES$^+$ and Me-8-ES$^+$ complexes, respectively. These results reflect that the bond length $d_{O\cdots H}$ gradually increases while binding energy ΔE_{int} ($\Delta E_{int,cp}$) and charge transfer $Q_{MULLIKEN}$ (Q_{NBO}) decrease from Me-2-ES$^+$ complex to Me-8-ES$^+$ complex. However, the change of these binding properties caused by increasing 2 phenyl rings are less significant when starting from complexes with more phenyl ring in the oligoaniline, for example, the difference between bond length $d_{O\cdots H}$ of Me-8-ES$^+$ and Me-6-ES$^+$ is 0.018 Å which is less significant than that of Me-6-ES$^+$ and Me-4-ES$^+$ (0.023 Å), which is again less significant than that of Me-4-ES$^+$ and Me-2-ES$^+$ (0.034 Å), implying that the increase in chain length has less effect in long chain complexes. A comprehensive theoretical investigation on properties of PANI n-ES$^+$ with different chain length was reported [26]. The authors concluded that n-ES$^+$ with seven building blocks can be used to describe the cationic defects in the polymer. Considering computational time, we think the cationic oligoaniline containing 8 repeating units can be used to model single PANI fiber to study its response mechanism to alcohol.

Both of the dihedral angle $\angle C_2C_3N_{23}C_{10}$ and torsion angle T in Me-8-ES$^+$, as well as all of the other Me-n-ES$^+$ (n = 2, 4, 6) complexes, are smaller than those in the corresponding oligoanilines, revealing that the adjacent phenyl rings in oligoaniline are more coplanar when exposing to methanol. So the transference of electrons along the oligoaniline chain becomes easier, resulting in resistance reduce in PANI. This is consistent with the experimental results of single PANI nanofiber sensor [16] and proposed mechanism for response of PANI to methanol [10].

Optimized geometries (Fig. 1S, 2S and 3S) and interactions between oligoanilines and ethanol, propanol as well as isopropanol are summarized in Support information (Tables 1S, 2S and 3S), respectively. Based on results listed in Tables 1S, 2S and 3S, the increase in oligoaniline chain length of Et-(2x + 2)-ES$^+$, Pr-(2x + 2)-ES$^+$ and *i*Pr-(2x + 2)-ES$^+$ complexes has similar influence as that of their methanol counterpart Me-(2x + 2)-ES$^+$ on the binding properties of the complexes, including $d_{O\cdots H}$ bond length, charge transfer and energy. For example, in a series of Et-(2x + 2)-ES$^+$, Pr-(2x + 2)-ES$^+$ and *i*Pr-(2x + 2)-ES$^+$ complexes (x = 0, 1, 2, 3), the bond lengths $d_{O\cdots H}$ gradually increases when the number of phenyl rings in oligoaniline increases from 2 to 4, 6 and 8 (corresponding to x = 0, 1, 2, and 3), while both the Mulliken and the NBO charge distribution gradually decrease. The values of both of energetic stabilities ΔE_{int}

Table 3
Intermolecular parameters of methanol-(2x + 2)-ES$^+$ complex ($d_{O\cdots H}$ in Å, ∠N—H…O and the dihedral angle $\angle C_2C_3N_{23}C_{10}$ in deg, respectively) obtained at UB3LYP/6-31g (d) level, noncorrected and couterpoise corrected interaction energies (ΔE_{int} and $\Delta E_{int,cp}$ in kcal/mol), NBO and ESP charges of Me-(2x + 2)-ES$^+$ complexes obtained at UB3LYP/6-311++g (d, p) level. The first column x refers to the length of the PANI-ES. Refer to Fig. 2(a) for atomic labels.

x	$d_{O\cdots H}$	∠NH…O	ΔE_{int}	$\Delta E_{int,cp}$	Q_{NBO}	$Q_{MILLKEN}$	$\angle C_2C_3N_{23}C_{10}$
0	1.845	180.0	−30.6	−29.7	0.034	0.020	−21.58(−22.41)
1	1.879	179.7	−28.6	−27.7	0.030	0.019	−21.67(−22.63)
2	1.902	174.4	−27.3	−26.4	0.026	0.015	−22.35(−23.22)
3	1.920	179.3	−26.4	−25.5	0.025	0.011	−22.57(−24.20)

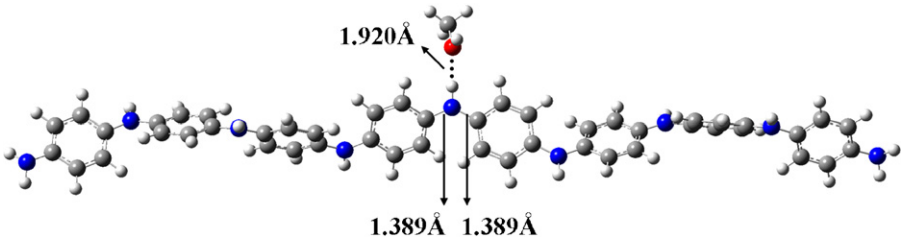

Fig. 3. Optimized geometry of methanol-8-ES$^+$ complex calculated at UB3LYP/6-31G (d) level. Refer to Fig. 2(a) for atomic labels.

and $\Delta E_{int,cp}$ greatly reduce as well. Again, the change of the binding properties caused by increasing 2 phenyl rings is less significant when starting from the complexes with more phenyl ring in the oligoaniline. Therefore, cationic oligoaniline containing 8 repeating units can also be used to model single PANI fiber response mechanism for ethanol, propanol and isopropanol.

Both of the dihedral angle $\angle C_2C_3N_{23}C_{10}$ and torsion angle T of 8-ES$^+$ decrease upon complexing with ethanol, propanol and isopropanol, indicating that the adjacent phenyl rings in oligoaniline are more coplanar when exposing to the alcohols. That is, the transference of electrons along the oligoaniline chain is facilitated and the resistance of PANI reduces. The decrease in resistance of the single PANI nanofiber sensor was detected when it exposed to ethanol and isopropanol [16]. The resistance reducing was explained by the authors to be due to the interaction of the alcohol with nitrogen atoms of PANI, resulting in an extended chain conformation which facilitating charge transport [16]. An response mechanism of PANI to small size alcohols can be proposed consequently that due to ion–dipole interaction forming O…H bond between polymer and small alcohols, the coplanarity of two adjacent phenyl rings in the polymer obviously increase, which facilitates electron transfer along the polymer chain and is responsible for the reduction of resistance of the polymer.

4. Conclusions

Binding properties of complexes of oligoanilines $(2x+2)$-ES$^+$ with methanol, ethanol, propanol and isopropanol were not obviously influent when oligoanilines chain length increase from 2 to 8. So to save computational time, cationic oligoaniline containing 8 repeating units can be used to model single PANI fiber to study its response mechanism to the alcohols. Upon complexing with methanol, ethanol, propanol and isopropanol, the ion–dipole interaction forms and result in the torsion of two adjacent phenyl rings in oligoaniline decreases. A response mechanism of PANI to small size alcohols can be proposed consequently that the high degree in coplanarity of two adjacent phenyl rings in the polymer caused by the alcohols is responsible for the reduction of resistance of the polymer as electron transfer along the polymer chain are facilitated.

Acknowledgment

This work was supported by the National Natural Science Foundation of China (Grants 50973013, 10874234, 20703064).

Appendix A. Supplementary data

Supplementary data associated with this article can be found, in the online version, at http://dx.doi.org/10.1016/j.synthmet.2012.03.015.

References

[1] J.W.Y. Lam, B.Z. Tang, Acc. Chem. Res. 38 (2005) 745.
[2] J.N. Barisci, J. Mansouri, G.M. Spinks, G.G. Wallace, C.Y. Kim, D.Y. Kim, J.Y. Kim, Colloid Surf. A: Physicochem. Eng. Asp. 126 (1997) 129.
[3] B. Wang, M.R. Wasielewski, J. Am. Chem. Soc. 119 (1997) 12.
[4] D.T. McQuade, A.E. Pullen, T.M. Swager, Chem. Rev. 100 (2000) 2537.
[5] J.X. Huang, S. Virji, B.H. Weiller, R.B. Kaner, J. Am. Chem. Soc. 125 (2003) 314.
[6] J. Janata, M. Josowicz, Nat. Mater. 2 (2003) 19.
[7] H. Spanggaard, F.C. Krebs, Sol. Energy Mater. Sol. Cells 83 (2004) 125.
[8] A.G. MacDiarmid, Angew. Chem.: Int. Ed. 40 (2001) 2581.
[9] H.L. Li, J.X. Wang, Q.X. Chu, Z. Wang, F.B. Zhang, S.C. Wang, J. Power Sources 190 (2009) 578.
[10] S. Virji, J.X. Huang, R.B. Kaner, B.H. Weiller, Nano Lett. 4 (2004) 491.
[11] L.J. Bian, J.H. Zhang, J. Qi, X.X. Liu, D. Dermot, K.T. Lau, Sens. Actuator B: Chem., 147 (2010), 73.
[12] F.W. Zeng, X.X. Liu, D. Diamond, K.T. Lau, Sens. Actuator B: Chem., 143 (2010), 530.
[13] S.H. Hosseini, A.A. Entezami, Polym. Adv. Technol. 12 (2001) 482.
[14] R.A. Potyrailo, C. Surman, S. Go, Y. Lee, T. Sivavec, W.G. Morris, J. Appl. Phys. 106 (2009) 6.
[15] W. Li, N.D. Hoa, Y. Cho, D. Kim, J.S. Kim, Sens. Actuator B: Chem. 143 (2009) 132.
[16] N.J. Pinto, I. Ramos, R. Rojas, P.C. Wang, A.T. Johnson, Sens. Actuator B: Chem. 129 (2008) 621.
[17] A. Calderone, R. Lazzaroni, J.L. Bredas, Phys. Rev. B (Condens. Matter) 49 (1994) 14418.
[18] J. Libert, J.L. Bredas, Seoul, South Korea, 1994 (unpublished).
[19] R. Hey, M. Schreiber, J. Chem. Phys. 103 (1995) 10726.
[20] P. Barta, T. Kugler, W.R. Salaneck, A.P. Monkman, J. Libert, R. Lazzaroni, J.L. Bredas, Synth. Met. 93 (1998) 83.
[21] M.I. Boyer, S. Quillard, E. Rebourt, G. Louarn, J.P. Buisson, A. Monkman, S. Lefrant, J. Phys. Chem. B 102 (1998) 7382.
[22] M. Cochet, G. Louarn, S. Quillard, J.P. Buisson, S. Lefrant, J. Raman Spectrosc. 31 (2000) 1041.
[23] M. Can, N.O. Pekmez, A. Yildiz, Polymer 44 (2003) 2585.
[24] Z. Cherrak, P. Lagant, N. Benharrats, A. Semmoud, F. Hamdache, G. Vergoten, Kansas City, MO, 2005.
[25] L.T. Sein, A.F. Lashua, Synth. Met. 159 (2009) 1183.
[26] C. Alemán, C.A. Ferreira, J. Torras, A. Meneguzzi, M. Canales, M.A.S. Rodrigues, J. Casanovas, Polymer 49 (2008) 5169.
[27] J. Libert, J. Cornil, D.A. dosSantos, J.L. Bredas, Phys. Rev. B 56 (1997) 8638.
[28] C.H. Choi, M. Kertesz, M.I. Boyer, M. Cochet, S. Quillard, G. Louarn, S. Lefrant, Chem. Mater. 11 (1999) 855.
[29] S.A. Jansen, T. Duong, A. Major, Y. Wei, L.T. Sein, Synth. Met. 105 (1999) 107.
[30] U. Salzner, T. Kiziltepe, J. Org. Chem. 64 (1999) 764.
[31] M.E. Vaschetto, B.A. Retamal, A.P. Monkman, Theochem. J. Mol. Struct. 468 (1999) 209.
[32] S.L. Lim, K.L. Tan, E.T. Kang, W.S. Chin, J. Chem. Phys. 112 (2000) 10648.
[33] L.T. Sein, T. Duong, Y. Wei, S.A. Jansen, Synth. Met. 113 (2000) 145.
[34] L.T. Sein, Y. Wei, S.A. Jansen, J. Phys. Chem. A 104 (2000) 11371.
[35] L.T. Sein, Y. Wei, S.A. Jansen, Synth. Met. 126 (2002) 117.
[36] J.P. Foreman, A.P. Monkman, J. Phys. Chem. A 107 (2003) 7604.
[37] N.A. Zaidi, J.P. Foreman, G. Tzamalis, S.C. Monkman, A.P. Monkman, Adv. Funct. Mater. 14 (2004) 479.
[38] G. Yang, W.H. Hou, X.M. Feng, X.F. Jiang, J. Guo, Adv. Funct. Mater. 17 (2007) 3521.
[39] L.T. Sein, J. Phys. Chem. A 112 (2008) 2598.
[40] J. Casanovas, M. Canales, C.A. Ferreira, C. Aleman, J. Phys. Chem. A 113 (2009) 8795.
[41] A.D. Becke, J. Chem. Phys. 98 (1993) 1372.
[42] C. Lee, W. Yang, R.G. Parr, Phys. Rev. B 37 (1988) 785.
[43] S.F. Boys, F. Beranrdi, Mol. Phys. 19 (1970).
[44] A.E. Reed, R.B. Weinstock, F. Weinhold, J. Chem. Phys. 83 (1985) 735.
[45] A.E. Reed, L.A. Curtiss, F. Weinhold, Chem. Rev. 88 (1988) 899.
[46] J.E. Carpenter, F. Weinhold, J. Mol. Struct.: Theochem. 169 (1988) 41.
[47] M.J. Frisch, G.W. Trucks, H.B. Schlegel, G.E. Scuseria, M.A. Robb, J.R. Cheeseman, G., Scalmani, V., Barone, B., Mennucci, G.A. Petersson, H., Nakatsuji, M., Caricato, X., Li, H.P. Hratchian, A.F. Izmaylov, J., Bloino, G., Zheng, J.L. Sonnenberg, M.,

Hada, M., Ehara, K., Toyota, R., Fukuda, J., Hasegawa, M., Ishida, T., Nakajima, Y., Honda, O., Kitao, H., Nakai, T., Vreven, J.A. Montgomery, Jr., J.E. Peralta, F., Ogliaro, M., Bearpark, J.J. Heyd, E., Brothers, K.N. Kudin, V.N. Staroverov, R., Kobayashi, J., Normand, K., Raghavachari, A., Rendell, J.C. Burant, S.S. Iyengar, J., Tomasi, M., Cossi, N., Rega, J.M. Millam, M., Klene, J.E. Knox, J.B. Cross, V., Bakken, C., Adamo, J., Jaramillo, R., Gomperts, R.E. Stratmann, O. Yazyev, A.J. Austin, R. Cammi, C. Pomelli, J.W. Ochterski, R.L. Martin, K. Morokuma, V.G. Zakrzewski, G.A. Voth, P. Salvador, J.J. Dannenberg, S. Dapprich, A.D. Daniels, O. Farkas, J.B. Foresman, J.V. Ortiz, J. Cioslowski, D.J. Fox. Gaussian 09, Revision A.02, Gaussian, Inc., Wallingford CT, 2009.

[48] T.M. Krygowski, W.R. Fawcett, J. Am. Chem. Soc. 97 (1975) 2143.

[49] M. Hara, A. Eisenberg, Macromolecules 17 (1984) 1335.

[50] X. Zou, H. Bao, H. Guo, L. Zhang, L. Qi, J. Jiang, L. Niu, S. Dong, J. Colloid Interface Sci. 295 (2006) 401.